

# Self-Assembly Molecular Dynamics Simulations Shed Light into the Interaction of the Influenza Fusion Peptide with a Membrane Bilayer

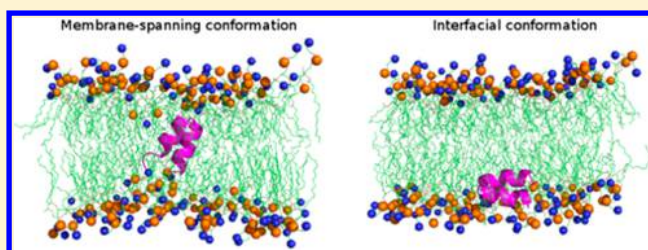
Bruno L. Victor,<sup>†</sup> Diana Lousa, Jorge M. Antunes, and Cláudio M. Soares\*

ITQB, Instituto de Tecnologia Química e Biológica António Xavier, Universidade Nova de Lisboa, Av. da República, 2780-157 Oeiras, Portugal

## Supporting Information

**ABSTRACT:** Influenza virus is one of the most devastating human pathogens. In order to infect host cells, this virus fuses its membrane with the host membrane in a process mediated by the glycoprotein hemagglutinin. During fusion, the N-terminal region of hemagglutinin, which is known as the fusion peptide (FP), inserts into the host membrane, promoting lipid mixing between the viral and host membranes. Therefore, this peptide plays a key role in the fusion process, but the exact mechanism by which it promotes lipid mixing is still unclear.

To shed light into this matter, we performed molecular dynamics (MD) simulations of the influenza FP in different environments (water, dodecylphosphocholine (DPC) micelles, and a dimyristoylphosphatidylcholine (DMPC) membrane). While in pure water the peptide lost its initial secondary structure, in simulations performed in the presence of DPC micelles it remained stable, in agreement with previous experimental observations. In simulations performed in the presence of a preassembled DMPC bilayer, the peptide became unstructured and was unable to insert into the membrane as a result of technical limitations of the method used. To overcome this problem, we used a self-assembly strategy, assembling the membrane together with the peptide. These simulations revealed that the peptide can adopt a membrane-spanning conformation, which had not been predicted by previous MD simulation studies. The peptide insertion had a strong effect on the membrane, lowering the bilayer thickness, disordering nearby lipids, and promoting lipid tail protrusion. These results contribute to a better understanding of the role of the FP in the fusion process.



## INTRODUCTION

Influenza virus is responsible for hundreds of thousands of deaths every year. The situation becomes even worse in pandemic years, when a subtype that was not previously circulating emerges and spreads among the human population. Influenza is therefore a major health concern, and the development of effective drugs against this virus is one of the biggest quests of modern medicine.

Like all enveloped viruses, influenza is covered by a lipid membrane (envelope), and in order to infect host cells it fuses its membrane with the membrane of the host cell. This fusion process is mediated by the glycoprotein hemagglutinin (HA) (for a recent review of this subject, see ref 1). This protein is a homotrimer, and each monomer is composed of two different subunits (HA1 and HA2). The fusion machinery is located in HA2, while HA1 is responsible for recognition and binding to the host cell.<sup>1,2</sup> After binding to the host cell surface, influenza virus is engulfed by endocytosis, becoming enclosed inside an endosome. The acidic pH of the late endosome triggers a large conformational change in the structure of HA, exposing the N-terminal region of HA2. This region, also known as the fusion peptide (FP), inserts into the host membrane,<sup>1–3</sup> promoting its destabilization and later on the fusion with the membrane of the virus.

The role of the fusion peptide has been studied both in the context of the complete HA protein and by using isolated FP segments (see refs 3 and 4 for reviews). These individual segments are able to promote lipid mixing between different liposomes and destabilize membrane bilayers.<sup>4,5</sup> Thus, the isolated FP can be used as model to study the interaction between this region of HA and lipid membranes.

One of the advantages of using isolated FP fragments is that they can be used to study the structure of this region in lipidic environments. Therefore, several NMR structures of the FP solubilized in dodecylphosphocholine (DPC) micelles have been determined.<sup>6–11</sup> In the first study of this kind, the authors solved the structure of the H3 subtype FP.<sup>11</sup> They used an FP segment comprising only the first 20 amino acid residues of the HA2 subunit, which was found to have a V-shaped conformation at the endosome pH. However, the use of only the first 20 amino acid residues raised some concerns,<sup>7</sup> since residues 21–23 are strictly conserved across all serotypes of HA. Additionally, mutations in W21 and Y22 have been shown to result in negative fusion phenotypes,<sup>3</sup> which shows that these residues are important for the FP function.

Received: December 20, 2014

Published: March 31, 2015

In order to analyze the effect of including residues 21–23 on the FP structure, Lorieau et al.<sup>7</sup> solved the NMR structure of the full length FP (comprising residues 1–23) from the H1 subtype. They found that this peptide adopts a helical hairpin structure in which two antiparallel helices are connected by a tight hairpin turn (see Figure 1B). This conformation is considerably more closed than the previous V-shaped structure,<sup>11</sup> which indicates that the peptide length influences its structure.<sup>7</sup> The close packing is allowed because of the existence of a glycine zipper formed by two pairs of glycine residues, with each glycine residue of one helix facing a glycine residue of the other helix. The hairpin structure is also stabilized by close contacts between residues 21–23 and the N-terminal residues, which explains the influence of the last three residues on the peptide conformation. The hypothesis that the peptide length influences its structure was further supported in a following study performed by the same authors.<sup>9</sup> In that study, they solved the structure of fusion peptides of different lengths and subtypes and concluded that shorter peptides lack key interactions that stabilize the closed helical-hairpin structure.<sup>9</sup>

Despite the large number of studies devoted to the study of the FP, the mechanism of action of this peptide remains unclear. Several mechanisms have been suggested, such as the induction of local disorder, promotion of membrane curvature, or alteration of local membrane composition.<sup>4,12</sup> A possible mechanism has been proposed by a molecular dynamics (MD) simulation study in which the authors simulated the fusion process of lipid vesicles.<sup>13</sup> They found that the transition state of this process is defined by the contact of a few lipid tails from the fusing vesicles. This contact occurs when lipid tails protrude into the hydrophilic region, which indicates that this event is determinant for the fusion process. In the same study, the authors performed simulations of the influenza FP in lipid membranes and found that the peptide promotes lipid tail protrusion in nearby lipids<sup>13</sup> (which has also been observed in other MD simulation studies<sup>14,15</sup>). These results suggest that the fusion peptide accelerates the fusion process by inducing lipid tail protrusion.<sup>13,16</sup> Recent results suggest that the FP not only induces lipid tail protrusion but also promotes polar head intrusion, i.e., sinking of nearby lipid headgroups.<sup>15</sup>

Other MD simulation studies have also tried to elucidate how the influenza and other viral fusion peptides, such as the fusion peptide from HIV gp41, insert into and interact with lipid membranes.<sup>13,14,17–31</sup> In most of these studies, the authors used either an implicit model for the lipid bilayer or a pre-equilibrated membrane in which the peptide was inserted. In most cases the V-shaped structure obtained by Han et al.<sup>11</sup> using only the first 20 amino acid residues of HA2 was employed, and this structure was found to be stable in the membrane. In a recent study, MD simulations using the closed hairpin structure of the full-length influenza FP and an explicit membrane bilayer were performed.<sup>23</sup> In these simulations the peptide was stable and remained close to the lipid phosphate groups. However, one should keep in mind that the membrane is a very viscous environment. Therefore, the insertion depth, orientation, and structure of the peptide are constrained and are not expected to change considerably in the time scale available to current standard MD simulations. Because of these limitations, the results obtained in previous MD studies may reflect the initial choices that were made regarding the structure and insertion of the peptide.

In order to shed light into the role played by the FP in the fusion process, we analyzed this peptide by performing MD simulations. The main goal of this work was to determine the orientation, insertion depth, and structure of the influenza FP in a membrane. To answer these questions, besides more conventional studies, we adopted an innovative approach by using a self-assembly protocol in which the peptide, lipid, and water molecules were initially randomly distributed in the simulation box. The self-assembly simulations showed, in the majority of replicates, a membrane spanning conformation for the fusion peptide, something that has never been observed before. Moreover, our results support the hypothesis that the FP induces lipid mixing by promoting intrusion of the head groups and protrusion of the lipid tails.

## METHODS

### Selection of Peptide Structure and Protonation State.

In this work, we used the H1 subtype FP structure obtained by Lorieau et al.<sup>7</sup> in the presence of DPC micelles. We chose this structure not only because it is one of the most recent structures of the influenza FP but also because the authors characterized the full-length FP containing the first 23 amino acid residues of the HA2 subunit (HAfp<sup>1–23</sup>) (the location of the FP in the prefusion structure of HA is shown in Figure 1A).

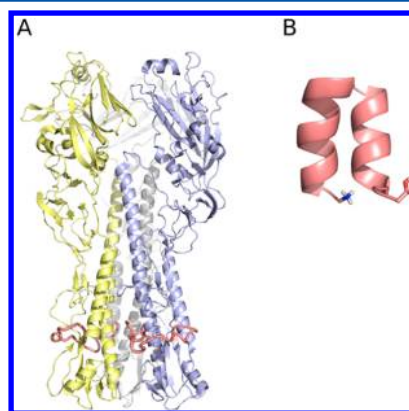


**Figure 1.** Structure of the influenza fusion peptide in the prefusion and fusion states. In the prefusion state, the FP is inserted into a hydrophobic pocket located on the bottom region of HA. The location of the fusion peptide in the prefusion structure of hemagglutinin (PDB ID 1RUZ) is shown in panel A. The protein backbone is displayed using a cartoon representation, with each monomer represented in a different color and the fusion peptide highlighted in pink. It is believed that the structure of the FP changes in going from the prefusion to the fusion state, when it inserts into the host membrane. The conformation of the membrane-inserted FP is proposed to be similar to the NMR structure obtained in DPC micelles,<sup>7</sup> which is displayed in panel B. A cartoon representation is used for the peptide backbone, and the N- and C-terminus are represented in sticks, with carbon, nitrogen, oxygen, and hydrogen atoms colored in pink, blue, red, and white, respectively.

To determine the NMR structure, the authors expressed HAfp<sup>1–23</sup> flanked by the residues SGKKKKD at its C-terminus in order to increase the peptide solubility. The structure of the peptide determined in micelles, which is thought to be representative of the conformation adopted when the peptide is in the host membrane, is depicted in Figure 1B. In our work, we truncated the peptide after Ser24. Although this residue is not part of the FP sequence, we maintained it in order to create

Table 1. Description of the Simulated Systems

simulation set	composition of the system	total no. of atoms	protonation state of E11 and D19	simulation time (ns)	no. of replicates
FP in water at low pH	FP + water	19640	both residues protonated	500	3
FP in water at neutral pH	FP + water	19637	both residues deprotonated	500	3
FP in the presence of a DPC micelle	FP + DPC + water	44658	both residues protonated	500	3
FP in the presence of a preassembled membrane with 128 DMPC	FP + DMPC + water	19753	both residues protonated	500	6
FP in the presence of a preassembled membrane with 125 DMPC	FP + DMPC + water	19523	both residues protonated	500	6
membrane self-assembly around the FP under isotropic conditions	FP + DMPC + water	24367	both residues protonated	variable (see Table 2)	10 simulated replicates (five were productive)
self-assembled systems under semi-isotropic conditions	FP + DMPC + water	24367	both residues protonated	400	5

a cap for the FP, which under biological conditions is attached to the rest of the protein by its C-terminus.

In this study, we aimed to simulate the FP at the pH of late endosomes, when fusion occurs, which is  $\sim 4\text{--}5$ . We considered both the N-terminus (which is the real N-terminus of hemagglutinin HA2) and the C-terminus to be protonated. The C-terminus of Ser24 was considered protonated because it was used as a cap, mimicking the rest of the protein. HAfp<sup>1–23</sup> has only two residues whose protonation state at pH 4 is not obvious: Glu11 and Asp19. According to the study by Lorieau et al.,<sup>7</sup> both residues are protonated at pH 4. Thus, in micelle and membrane simulations, in order to mimic the experimental conditions, we protonated both these amino acid residues. In the case of the simulations performed solely in water, we tested two protonation conditions: low pH (with Glu11 and Asp19 protonated) and high pH (with the two residues deprotonated) (see Table 1).

#### General Setup for Molecular Dynamics Simulations.

In order to analyze the properties of the FP under different conditions, we performed different sets of simulations, which are described in Table 1. All of the simulations were performed with the GROMACS 4.0.4 software package<sup>32,33</sup> using the GROMOS 54A7 force field (FF)<sup>34</sup> and the SPC water model.<sup>35</sup> The dimyristoylphosphatidylcholine (DMPC) parameters were taken from ref 36, and the charges derived by Chiu et al.<sup>37</sup> were used. For the simulations with DPC molecules, the parameters used for the polar groups were the same as those used for DMPC,<sup>36</sup> and the aliphatic carbons were modeled using the GROMOS 54A7 parameters.<sup>34</sup> The bond length of the water molecules was constrained with the SETTLE algorithm,<sup>38</sup> while the bonds of the FP and lipid molecules were constrained using LINCS.<sup>39</sup> The time step used for integration in all of the simulations was 2 fs. In the simulations with the DMPC bilayer, we used a tetragonal unit cell with periodic boundary conditions (PBCs), and for the simulations with DPC micelles and aqueous systems, we used a rhombic dodecahedron with PBCs. The simulations were performed in the *NPT* ensemble, using the Berendsen heat and pressure baths<sup>40</sup> to keep the temperature and pressure constant. The temperature was kept at 310 K in membrane simulations and 300 K in aqueous and micelle simulations. Separate heat baths were used to couple the FP, solvent molecules, and lipids, with a relaxation time constant of 0.1 ps. In the aqueous and DPC micelle simulations, we used an isotropic pressure coupling at 1 bar with relaxation time constants of 1 and 0.5 ps for water and DPC simulations, respectively, and a compressibility of  $4.5 \times$

$10^{-5} \text{ bar}^{-1}$ . In the simulations with the membrane, we used a semi-isotropic pressure coupling (except in the self-assembly protocol; see the Supporting Information) with a relaxation time constant of 1 ps and a compressibility of  $4.5 \times 10^{-5} \text{ bar}^{-1}$ . A twin-range cutoff of 8 and 14 Å for short and long-range interactions was used, respectively, and the neighbor list was updated every five steps.<sup>41</sup> Long-range electrostatic interactions were treated with the reaction field method<sup>42</sup> with a dielectric constant of 54.<sup>43</sup> For each simulation set, we performed at least three replicate simulations, although in some specific cases more replicates were considered (see Table 1).

The specific details of the setup and equilibration of each study (FP peptide in water, FP peptide in a micelle, FP peptide in preassembled membranes, and membrane self-assembly with the FP peptide) can be found in the Supporting Information.

## RESULTS AND DISCUSSION

**Simulations of the FP in Water.** Since the FP is exposed to an aqueous environment before it inserts into the host membrane, we started by performing simulations in pure water. Given that pH plays a key role in triggering the fusion process and affects the activity of the FP,<sup>44</sup> we performed two sets of MD simulations in water considering two different protonation conditions (E11 and D19 protonated vs E11 and D19 deprotonated; see Table 1).

The NMR structure determined by Lorieau et al. in DPC micelles<sup>7</sup> was used as a starting point for the MD simulations. As can be seen in the final structures obtained in the water simulations (Figure 2), in most replicates the peptide became unstructured, independent of the protonation state considered. This is also clear in the time evolution of the root-mean-square deviation (RMSD) and the secondary structure plots, available in columns 2 and 3 of Figure S1 in the Supporting Information, respectively. These results indicate that the structure determined in a lipid-like environment is not stable in water, which is in agreement with previous circular dichroism analysis showing that the peptide is mostly unstructured in aqueous solution.<sup>5</sup>

#### Simulations of the FP in the Presence of a Micelle.

After analyzing the structural properties of the FP in aqueous solution, we wanted to study the peptide conformation in a lipidic environment. We started by performing simulations of the peptide in the presence of a previously assembled DPC detergent micelle. Given that the NMR structure of the FP used in this study was obtained in a DPC micelle, we can directly



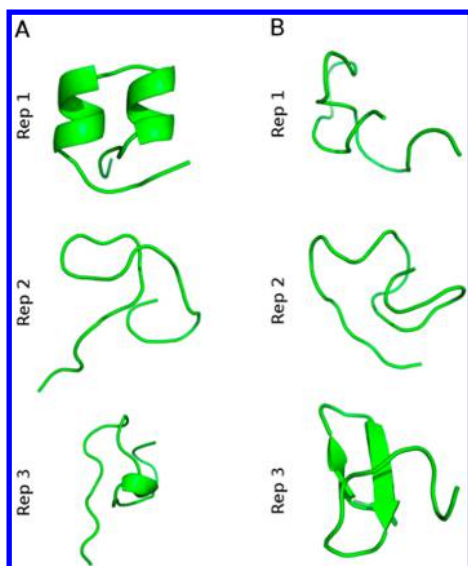


**Figure 2.** Final conformation of the FP in water simulations with E11 and D19 protonated (A) or deprotonated (B). For each replicate, the final conformation of the peptide is displayed using a cartoon representation, with carbon atoms colored in green.

compare the structural properties of the peptide in our simulations with those observed in the NMR structure.

We performed three replicate simulations starting with the peptide outside the DPC micelle, in close contact with the headgroups. In all of them, the peptide rapidly inserted inside the micelle, and as can be seen in Figure 3, it was completely immersed in the micelle at the end of the simulations. The RMSD and secondary structure analysis (Figure 3, columns 3 and 4, respectively) showed that the structure of the peptide in the simulations performed in micelles did not deviate considerably from the NMR structure determined in a similar environment.

In order to see which regions of the fusion peptide were more exposed to water, we analyzed the average number of peptide amide–water contacts in the last 300 ns of simulation (Figure 3, second column). Interestingly, the plots of the three replicate simulations were very consistent. In all three reported

situations, the most exposed residues were residues 1–4, 12–16, and 23, whereas residues 5–8 and 17–22 established none or very few water contacts. The first residue established a larger number of amide–water contacts because the amide of this group (N-terminal) has three protons and therefore can participate in three hydrogen bonds with water. The number of water contacts observed in our simulations is in very good agreement with the solvent hydrogen exchange rates of the backbone amide protons measured by Lorieau et al. (see Figure 4C in ref 7).

The results discussed in this section show that our simulations were able to reproduce the experimentally observed structural properties of the FP in a DPC micelle. This makes us confident that the force field and simulation setup that we used were appropriate for this study.

**Simulations of the FP in the Presence of a Preassembled Lipid Bilayer.** The main goal of this work was to analyze the influenza FP in a membrane bilayer, which is the natural situation (and not the detergent micelles where the NMR structures were obtained). We started by simulating the FP in the presence of a preassembled DMPC bilayer, placing the peptide on the membrane exterior. As can be observed in Figure 4A, in five out six replicates the peptide did not insert into the membrane. Thus, in most cases the peptide remained exposed to water during the simulations, becoming unstructured (see Figure S2 and the section entitled “Detailed description of the simulations of the FP in the presence of a preassembled lipid bilayer with 128 DMPC molecules” in the Supporting Information). As shown in Figure 4B, the insertion of the peptide seems to be facilitated when some lipids are removed in order to make room for the peptide, but even in this case, the probability of observing insertion of the peptide into the membrane is low (see Figure S3 and the section entitled “Detailed description of the simulations of the FP in the presence of a preassembled lipid bilayer with 125 DMPC molecules” in the Supporting Information). These results are not consistent with previous experimental findings obtained with different techniques, which show that the FP inserts completely into the membrane bilayer.<sup>11,45,46</sup>

The fact that the FP did not penetrate inside the preassembled membrane in most replicates is most likely due to sampling limitations. We suggest that the peptide is likely to

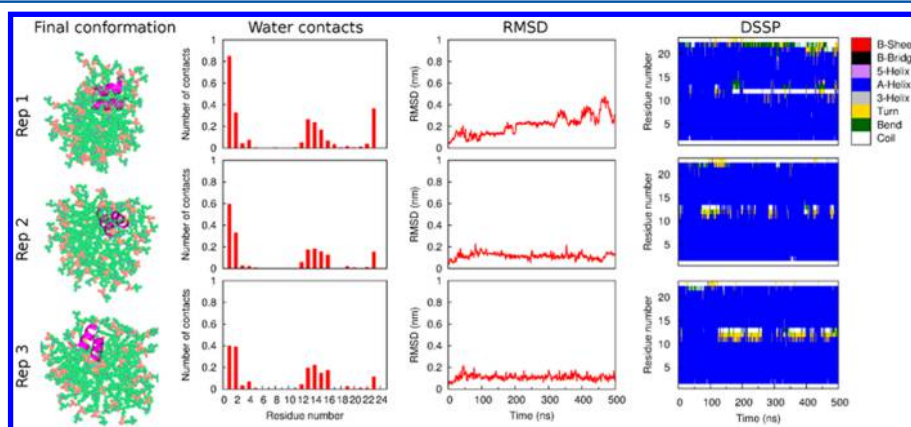


**Figure 3.** Structural properties of the FP in the presence of DPC micelles. For each replicate, the final conformation of the peptide (first column), the average number of water contacts (second column), the time evolution of the  $C\alpha$  RMSD computed against the NMR structure (third column), and the secondary structure content according to the DSSP criterion (fourth column) are displayed. The average number of water contacts was computed by counting the number of water molecules within 0.3 nm of the N-terminal atom of each residue in each frame and then averaging over the total number of frames (only the last 300 ns of simulation were used in the calculation).

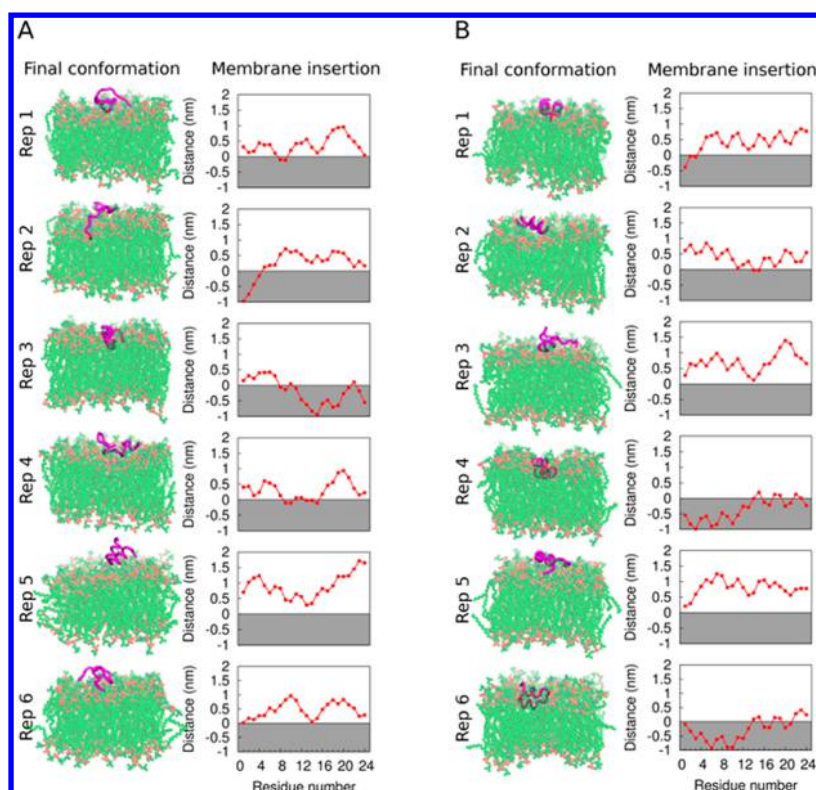


**Figure 4.** Conformations adopted by the FP in the presence of a preassembled membrane bilayer with 128 (A) or 125 (B) DMPC molecules. For each replicate, the final conformation of the peptide (first column) and the insertion depth of each residue in the last frame (second column) are displayed. The insertion depth was calculated by measuring the distance between the  $C\alpha$  atom of each residue and the average position of the phosphorus atoms in the monolayer that is closer to the peptide (positive values mean that the residue is on the membrane exterior, and negative values mean that the residue is in the membrane interior; a gray shadow is used to highlight the membrane interior).

enter the membrane in a random coil state (as evidenced by our studies in solution that show this conformation to be the one in water) and then folds into the two  $\alpha$ -helical structures observed experimentally in micelles. However, the time scale for this to happen is likely to be much longer than the one available to normal simulations with explicit solvent, especially if we consider the viscous and ordered environment of the membrane. This problem has been observed in previous simulations and has been discussed by Farrotti et al.<sup>47</sup> Therefore, we are now convinced that using a preassembled bilayer and waiting (within the available time scale of normal simulations) for the peptide to penetrate the membrane may not be an efficient strategy to analyze the conformation adopted by the peptide inside the membrane bilayer.

**Self-Assembly of a Lipid Bilayer around the FP under Isotropic Conditions.** To circumvent the limitations of the previous strategy, we decided to perform simulations in which the peptide, lipid, and water molecules were initially randomly distributed in the simulation box. Our aim was to let the lipids self-assemble to form a membrane bilayer and to determine the most stable position and arrangement of the peptide in this system. In the initial stages of the self-assembly protocol, the system is much more fluid than a preassembled membrane, which enables the peptide to explore a larger number of arrangements, increasing the probability of finding the most stable configuration. We note that although this protocol does not mimic the natural entry process of the peptide, it has been shown to be an efficient and unbiased way of determining the insertion mode of membrane-interacting peptides.<sup>48</sup> Moreover, predictions made with this type of simulation have been shown

to be in agreement with both experimental data and potential of mean force calculations,<sup>47</sup> which further supports the reliability of this method.

In our first tests, we tried to perform the self-assembly simulations under semi-isotropic conditions (applying the pressure coupling independently in the  $x$ - $y$  and  $z$  dimensions) because this is the most appropriate setup for membrane simulations. However, this protocol did not work (results not shown), and thus, we performed 10 replicate simulations under isotropic conditions. In this case, the membrane was able to spontaneously assemble in five out of the 10 replicates (productive replicates) in less than 1500 ns (Table 2). A movie showing the self-assembly of one of the simulations can be found in the Supporting Information.

**Table 2.** Time Required for Membrane Assembly and Tilt Angle of the Peptide in the Productive Self-Assembly Simulations

replicate	assembly time (ns)	tilt angle (deg) <sup>a</sup>
1	1400	62
2	1430	66
3	1190	30
4	470	7
5	325	50

<sup>a</sup>The tilt angle corresponds to the angle between the vector passing through the peptide N-terminal helix and the membrane plane. The value reported corresponds to an average over the last 100 ns of the simulation.

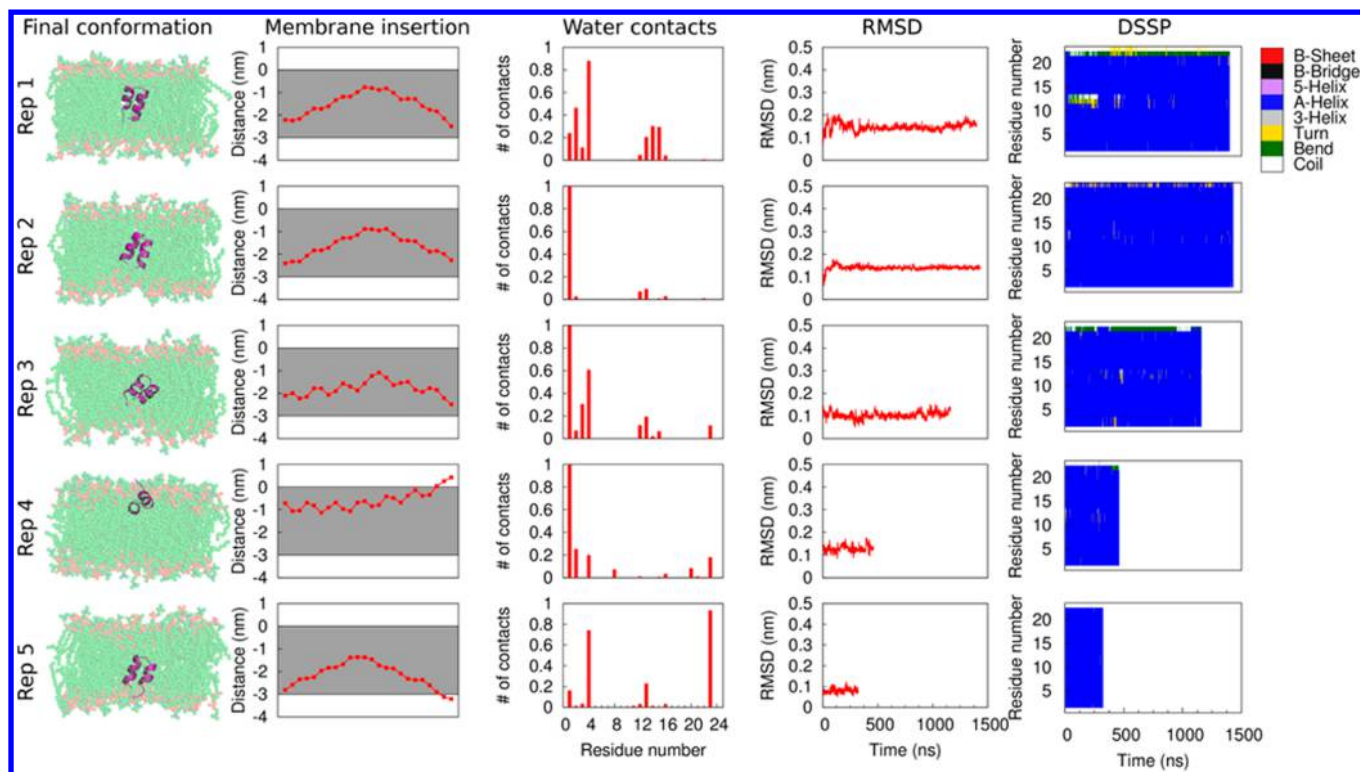


**Figure 5.** Structural properties of the FP in self-assembly simulations. For each productive self-assembly replicate, the final conformation of the peptide (first column), the insertion depth of each residue in the last frame (second column; see Figure 4 for a complete description), the average number of water contacts (third column; see Figure 3 for a complete description), the time evolution of  $\text{Ca}$  RMSD computed against the NMR structure (fourth column), and the secondary structure content according to DSSP (fifth column) are displayed.

As expected, in all of the productive replicates, the bilayer assembled around the peptide, which is consistent with previous experimental findings showing that the influenza FP inserts completely in the membrane.<sup>5,45,46</sup> In four out of the five productive replicates (replicates 1, 2, 3, and 5), the peptide became deeply inserted into the membrane and adopted a perpendicular or tilted orientation relative to the membrane plane, extending from one leaflet to the other and contacting the lipid headgroups on both sides of the membrane (see Table 2 and Figure 5). For the sake of simplicity, we will refer to this conformation as “membrane-spanning”.

This membrane-spanning configuration has not been observed in previous simulation studies, since in most of these studies the structure of the 20-residue peptide was used and the length of this peptide is not sufficient to span the membrane bilayer. In the only simulation study where the 23-residue FP structure was used,<sup>23</sup> the peptide was placed close to the lipid headgroups and remained there during the whole simulation. The fact that the peptide did not insert deeply into the membrane may be due to sampling limitations. Because of the high viscosity of the membrane, it is very hard to observe a large conformational rearrangement of the peptide inside the bilayer on the time scale available to current MD simulations. The self-assembly protocol used in this work enabled us to circumvent this limitation, and this explains why we were able to observe a conformation that had not been observed before.

In one of the productive replicates (replicate 4), the peptide was located at the interface between the headgroups and the lipid tails and adopted an approximately parallel orientation relative to the membrane plane (see Table 2 and Figure 5). The orientation adopted by the peptide in this replicate is similar to the orientations observed when the peptide inserted into a

preassembled bilayer with 125 lipids (replicates 4 and 6 in Figure 4B and Figure S3 in the Supporting Information). In all of these simulations the peptide inserted with similar tilt angles. The average tilt angles after insertion of the peptide in the simulations with the preassembled membrane were  $11^\circ$  and  $16^\circ$  for replicates 4 and 6, respectively, which are similar to the tilt angle of  $7^\circ$  observed in replicate 4 of the self-assembly simulations (Table 2). Moreover, in all cases, the C-terminal region of the peptide was more deeply inserted than the N-terminal region (see the insertion plots in Figure 4B (replicates 4 and 6) and Figure 5 (replicate 4)).

Overall, the results of the self-assembly simulations indicate that the FP can adopt different arrangements inside the membrane. This is consistent with NMR results showing that the orientation of HAFp<sup>1–23</sup> in the membrane is highly dynamic and that the peptide undergoes whole-body rocking motions.<sup>49</sup> Although the membrane-spanning conformation was the most predominant in the self-assembly simulations, we cannot claim that this conformation is the lowest free energy minimum. Nevertheless, it has been shown that this self-assembly protocol is able to correctly predict the most probable conformations of membrane-interacting peptides.<sup>48</sup> Thus, it is reasonable to say that the conformations found in this study represent possible and stable binding modes of the influenza FP.

The configurations obtained with the self-assembly protocol are compatible with previous experimental data showing that the peptide inserts completely inside the membrane.<sup>11,45,46</sup> Experimental studies using the 20-residue FP peptide (H3 subtype) indicated that at the fusion pH, the peptide adopts an inverted-V configuration in the membrane with the central region located in the lipid headgroup region and the N- and C-terminal helices inserted into the hydrophobic region of the



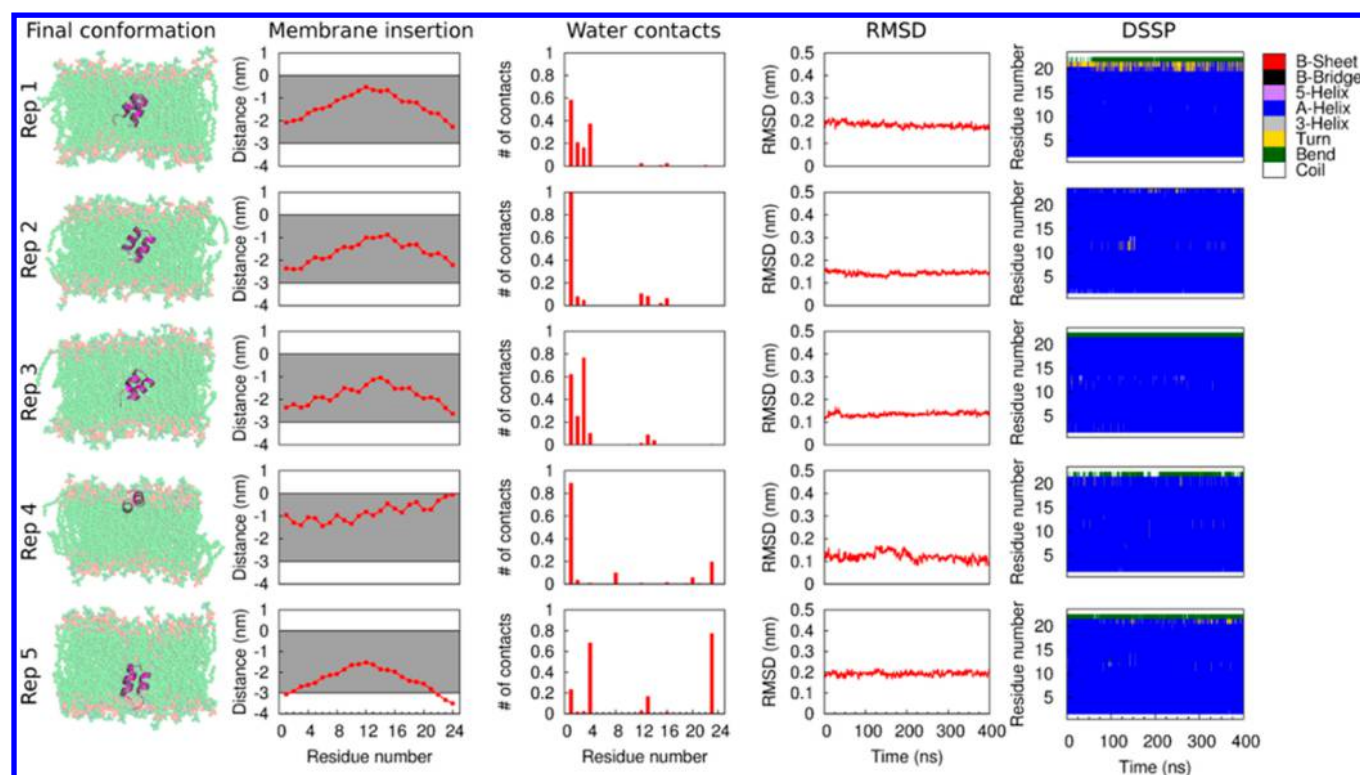


**Figure 6.** Structural properties of the FP in the simulations of the self-assembled systems under semi-isotropic conditions. The analyses displayed in this figure are identical to the ones described in Figure 5.

membrane.<sup>11</sup> Our results show some agreement with these observations, given that in four of the five replicates the central turn is located in the lipid headgroup region and the helices are deeply buried. The authors of the experimental study also determined the tilt angle between the N-terminal helix of the peptide and the plane of the membrane and obtained a value of  $\sim 38^\circ$ .<sup>11</sup> In our simulations we obtained different orientations of the FP, including one with a tilt angle similar to the one found by Han et al.<sup>11</sup> (replicate 3; see Table 2). We note, however, that these authors used a smaller FP segment than the one used in our simulations, which can strongly affect the structure and arrangement of the peptide inside the membrane. The 20-residue peptide is shorter and has a more open structure than the full-length peptide, and thus, it cannot span the membrane. Moreover, the experimental studies did not consider the fact that the peptide can pull the headgroups, causing the bilayer thickness to decrease, as has been observed in both the present and previous works<sup>18,19,50,51</sup> (see Figure 7). Therefore, although the peptide length is apparently not enough to span the membrane, the decrease in membrane thickness allows it to do so, and this could not have been predicted in the previous experimental studies. For this reason, the conformations observed in this work are plausible.

Lorieau et al.,<sup>7</sup> who determined the NMR structure used in the current study, analyzed the interaction of each residue with DPC and water molecules. They observed that residues 1–4, 12–13, and 21–23 interact more with the lipid polar headgroups and water molecules, whereas the rest of the peptide interacts with the hydrophobic tails of the lipids.<sup>7</sup> Although these results led the authors to propose that the peptide would insert into the headgroup–tail interface (similar to what is observed in replicate 4 in Figure 5), the results are

also consistent with an arrangement like the one observed in replicates 1, 2, 3, and 5.

Overall, the results of the self-assembly simulations are compatible with previous experimental findings, and even though we cannot claim that the conformations obtained in these simulations correspond to the lowest free energy minima, it is reasonable to say that they represent possible and stable binding modes of the influenza FP.

**Simulations of the Self-Assembled Systems under Semi-isotropic Conditions.** As mentioned before, it is common practice in membrane MD simulations to use a semi-isotropic pressure coupling because this allows the box to scale independently in the  $x$ – $y$  and  $z$  directions, which usually results in a more accurate description of the membrane properties, such as the area per lipid and volume per lipid. Moreover, the DMPC model used in our studies was parametrized under these conditions.<sup>36</sup> Thus, after assembling the membrane under isotropic conditions (which was the only way that we were able to obtain a well-assembled membrane bilayer around the peptide), we used the self-assembled systems to perform 400 ns of MD under semi-isotropic conditions.

As can be seen in columns 1 and 2 of Figure 6, the FP was still enclosed inside the membrane at the end of the semi-isotropic simulations, and the structure and orientation of the peptide did not change significantly in these simulations. The RMSD analysis (Figure 5, column 4) shows that the structure of the peptide did not deviate considerably from the reference structure (which is the NMR structure). Moreover, the secondary structure of the peptide remained predominantly helical during the simulations (Figure 6, column 5). These results indicate that the structure determined by Lorieau et al.<sup>7</sup> in DPC micelles is stable in a DMPC membrane.

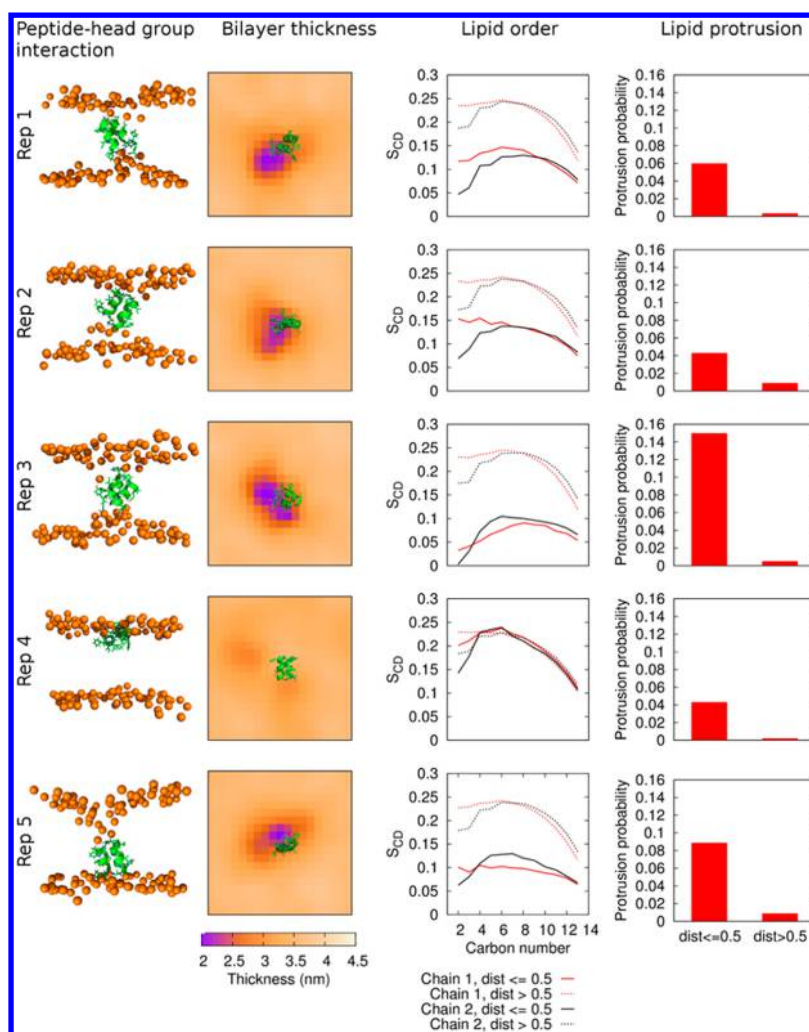


**Figure 7.** Interaction of the FP with a self-assembled DMPC membrane. For each productive self-assembly replicate, a molecular picture of the peptide interacting with the lipid headgroups in the last frame of the simulations performed under semi-isotropic conditions (first column), the bilayer thickness (second column), the order parameters for the sn-1 and sn-2 acyl tails of DMPC (third column), and the lipid protrusion probability (fourth column) are shown. The thickness of the bilayer was calculated using the Grid-MAT tool<sup>52</sup> and projected onto the *xy* plane. The structure of the peptide was superimposed on the thickness map to indicate its location. The order parameters were calculated with the g-order tool available in the GROMACS package.<sup>33</sup> The lipids were divided in two groups according to their average minimum distance to the peptide, and the order parameters were calculated separately for lipids within 0.5 nm of the peptide and for lipids outside of this region. Lipid protrusion was defined according to refs 6 and 7, i.e., any carbon in the lipid tail protruding more than 0.1 nm beyond the phosphate group was considered a protrusion event. Lipid protrusion was calculated separately for lipids within 0.5 nm of the peptide and for lipids outside this cutoff.

Because the peptide inserted into the membrane in all of the replicate simulations, most residues have a low number of contacts with water molecules (Figure 6, column 3). In most of the replicates, the peptide terminals and the kink region were more exposed to water than the rest of the peptide. Once again, this is consistent with the water–amide hydrogen exchange rates determined in ref 7.

One of the aims of this work was to analyze the molecular details of the interaction between the peptide and the host membrane. As can be seen in column 1 of Figure 7, it is clear that in the replicates in which the peptide is deeply inserted into the membrane, the polar groups of the peptide (mainly located in the kink region and in the termini) interact with the phosphate groups of the lipids. To analyze the effect of the peptide on the bilayer thickness, we calculated this property using the GridMAT tool,<sup>52</sup> which allows one to map the thickness on the *xy* plane of the membrane (Figure 7, column 2). In order to indicate the location of the peptide, which was

centered in the box before GridMAT was run, we superimposed the peptide structure on the thickness maps. This figure clearly shows that when the peptide is deeply inserted, it decreases the thickness in the surrounding area of the membrane, which has also been observed in previous MD simulation studies.<sup>18,19,50,51</sup> This is a consequence of the interaction with the phosphate groups and is consistent with the results of a recent MD simulation study in which the authors observed that the peptide promotes what they called “lipid polar head intrusion”.<sup>15</sup>

Some authors argue that the main role of the fusion peptide is to disturb the lipid membrane.<sup>12–14,19,53</sup> To analyze this hypothesis, we measured the order parameters of the sn-1 and sn-2 DMPC chains (Figure 7, column 3). As can be seen in the plots, in the replicates in which the peptide spans the membrane, the lipids close to the peptide are much more disordered than the rest of the membrane. This is in agreement with the findings of previous MD simulation studies.<sup>14,50,51</sup>



The same authors also found that the FP induces what they call “lipid tail protrusion” in the surrounding lipids.<sup>13,14</sup> According to these authors, this event occurs when the acyl chain of a lipid extends more than 0.1 nm over the phosphate group of the same lipid (Figure 8 illustrates a protrusion event

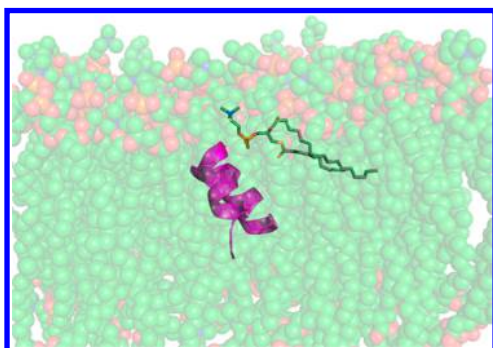


**Figure 8.** Lipid tail protrusion. The figure shows an acyl tail protruding in a snapshot taken from replicate 3 of the semi-isotropic simulations. The protruding lipid, which is close to the fusion peptide, is represented using sticks. One acyl tail of this lipid is bulging into the polar layer, extending >0.1 nm above its phosphate group, which meets the criterion used to define lipid protrusion (this criterion is the same as that used in refs 6 and 7).

found in our simulations). Lipid tail protrusion plays an important role in the fusion process due to an increase in the probability of contact between lipid tails from the fusing membranes.<sup>13,14</sup> We analyzed lipid tail protrusion in our simulations and found that the probability of this event is considerably higher for lipid molecules within a distance of 0.5 nm from the FP (Figure 7, column 4). A protrusion event observed in our simulations is displayed in Figure 8, which shows a lipid whose phosphate group is interacting with the peptide, inducing the lipid tail to protrude above this group. This effect is more evident in replicate 3 (Figure 7, column 4), which is probably related to the orientation of the peptide in this simulation (the peptide is oriented obliquely relative to the membrane plane, with a tilt angle of  $\sim 27^\circ$ ). The effect is also observed in replicate 4, where the peptide does not span the whole membrane. These results strongly support the hypothesis that the FP promotes fusion by destabilizing the host membrane and inducing lipid tail protrusion.

We note that although the peptide strongly disturbs the membrane, the area per lipid and the order parameters of the lipids that are not in contact with the peptide are similar to the ones observed in the preassembled membrane used in this work (results not shown). Moreover, these properties are consistent with previous experimental and theoretical values,<sup>54</sup> indicating that the self-assembled membrane is in the biologically relevant fluid phase.

## CONCLUSIONS

The N-terminal region of hemagglutinin HA2 subunit, which is known as the fusion peptide (FP), inserts into the host membrane during fusion and plays an important role in this process. Since the interaction of the peptide with the host membrane is thought to be crucial for fusion, the main goal of this work was to study the peptide in the presence of a model bilayer.

We started by placing the peptide in the exterior of a preassembled membrane and observed that it was very difficult

for the peptide to maintain its helix–kink–helix arrangement and insert into the membrane, even when some lipids were removed from one leaflet.

To overcome these problems, we used a self-assembly strategy, where the peptide, lipids, and water molecules were randomly distributed in the simulation box. On the basis of the results of these self-assembly simulations, we propose that the influenza FP can adopt two different orientations: spanning the bilayer or lying parallel to the membrane plane at the headgroup–lipid tail interface. In both configurations the C-terminal region of the peptide is located in the headgroup region. Therefore, these arrangements are consistent with the biological situation, in which the C-terminus of the peptide is attached to the rest of the protein, which does not insert into the hydrophobic core of the membrane (Figure 9).<sup>45</sup>

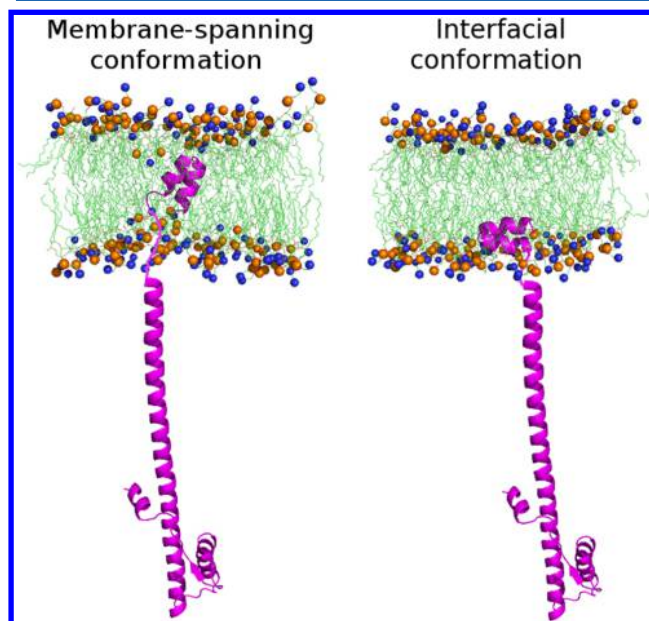


**Figure 9.** Model of the interaction of the FP with the host membrane in a biological context. The figure shows the final snapshots of two replicates in which the peptide adopted two distinct conformations: membrane-spanning (replicate 1) and interfacial (replicate 4). The structure of the HA2 subunit at the fusion pH (PDB ID 1HTM) is displayed to show how the peptide can be attached to the rest of the protein (we note that only the FP comprising the first 23 residues of HA2 was simulated). For the sake of simplicity, only one monomer of HA2 is represented.

The membrane-spanning conformation is likely to play an important role during the fusion process, since our results show that when the peptide adopts this arrangement it has a much more pronounced effect on the membrane, substantially decreasing the bilayer thickness in the surrounding region and decreasing the order of the nearby lipids. Lipid tail protrusion is also enhanced in the replicates in which the peptide is deeply inserted, and this event has been shown to be determinant for membrane fusion.<sup>13,14</sup> One should keep in mind that when the fusion process takes place, several FP molecules become inserted into the host membrane simultaneously. Thus, many regions of the membrane may be perturbed at the same time, thereby facilitating the fusion process.

## ■ ASSOCIATED CONTENT

### ■ Supporting Information

Supplementary methods, including aqueous simulation setup, micelle simulation setup, preassembled membrane simulation setup, and membrane self-assembly simulation setup; supplementary results, including a detailed description of the simulations of the FP in the presence of a preassembled lipid bilayer with 128 DMPC molecules and a detailed description of the simulations of the FP in the presence of a preassembled lipid bilayer with 125 DMPC molecules; supplementary figures, including (S1) structural properties of the FP in water simulations with E11 and D19 protonated (A) or deprotonated (B), (S2) structural properties of the FP in the presence of a preassembled membrane bilayer with 128 DMPC molecules, (S3) structural properties of the FP in the presence of a preassembled membrane bilayer with 125 DMPC molecules, and (S4) time evolution of the number of main-chain–water hydrogen bonds in the simulations performed in the presence of preassembled membranes with (A) 128 and (B) 125 DMPC lipids; and a movie (AVI) showing the 1400 ns trajectory of the first productive replicate of the self-assembly simulations. This material is available free of charge via the Internet at <http://pubs.acs.org>.

## ■ AUTHOR INFORMATION

### Corresponding Author

\*E-mail: [claudio@itqb.unl.pt](mailto:claudio@itqb.unl.pt).

### Present Address

<sup>†</sup>B.L.V.: BSIM<sup>2</sup>, Biocant Park, Cantanhede, Portugal.

### Notes

The authors declare no competing financial interest.

## ■ ACKNOWLEDGMENTS

We acknowledge Dr. António M. Baptista for fruitful discussions during the development of the work and the Fundação para a Ciência e a Tecnologia, Portugal, for financial support through Grants PTDC/QUI-BIQ/114774/2009, PEst-OE/EQB/LA0004/2011, SFRH/BPD/29708/2006, and SFRH/BPD/92537/2013.

## ■ REFERENCES

- (1) Luo, M. Influenza Virus Entry. *Adv. Exp. Med. Biol.* **2012**, 726, 201–221.
- (2) Skehel, J. J.; Wiley, D. C. Receptor binding and membrane fusion in virus entry: The influenza hemagglutinin. *Annu. Rev. Biochem.* **2000**, 69, 531–569.
- (3) Cross, K. J.; Langley, W. A.; Russell, R. J.; Skehel, J. J.; Steinhauer, D. A. Composition and Functions of the Influenza Fusion Peptide. *Protein Pept. Lett.* **2009**, 16, 766–778.
- (4) Epand, R. M. Fusion peptides and the mechanism of viral fusion. *Biochim. Biophys. Acta* **2003**, 1614, 116–121.
- (5) Han, X.; Tamm, L. K. A host–guest system to study structure–function relationships of membrane fusion peptides. *Proc. Natl. Acad. Sci. U.S.A.* **2000**, 97, 13097–13102.
- (6) Lai, A. L.; Park, H.; White, J. M.; Tamm, L. K. Fusion peptide of influenza hemagglutinin requires a fixed angle boomerang structure for activity. *J. Biol. Chem.* **2006**, 281, 5760–5770.
- (7) Lorieau, J. L.; Louis, J. M.; Bax, A. The complete influenza hemagglutinin fusion domain adopts a tight helical hairpin arrangement at the lipid:water interface. *Proc. Natl. Acad. Sci. U.S.A.* **2010**, 107, 11341–11346.
- (8) Lorieau, J. L.; Louis, J. M.; Bax, A. Helical Hairpin Structure of Influenza Hemagglutinin Fusion Peptide Stabilized by Charge–Dipole Interactions between the N-Terminal Amino Group and the Second Helix. *J. Am. Chem. Soc.* **2011**, 133, 2824–2827.
- (9) Lorieau, J. L.; Louis, J. M.; Bax, A. Impact of Influenza Hemagglutinin Fusion Peptide Length and Viral Subtype on Its Structure and Dynamics. *Biopolymers* **2013**, 99, 189–195.
- (10) Lorieau, J. L.; Louis, J. M.; Schwieters, C. D.; Bax, A. pH-triggered, activated-state conformations of the influenza hemagglutinin fusion peptide revealed by NMR. *Proc. Natl. Acad. Sci. U.S.A.* **2012**, 109, 19994–19999.
- (11) Han, X.; Bushweller, J. H.; Cafiso, D. S.; Tamm, L. K. Membrane structure and fusion-triggering conformational change of the fusion domain from influenza hemagglutinin. *Nat. Struct. Biol.* **2001**, 8, 715–720.
- (12) Chernomordik, L. V.; Kozlov, M. M. Mechanics of membrane fusion. *Nat. Struct. Mol. Biol.* **2008**, 15, 675–683.
- (13) Kasson, P. M.; Lindahl, E.; Pande, V. S. Atomic-Resolution Simulations Predict a Transition State for Vesicle Fusion Defined by Contact of a Few Lipid Tails. *PLoS Comput. Biol.* **2010**, 6, No. e1000829.
- (14) Larsson, P.; Kasson, P. M. Lipid Tail Protrusion in Simulations Predicts Fusogenic Activity of Influenza Fusion Peptide Mutants and Conformational Models. *PLoS Comput. Biol.* **2013**, 9, No. e1002950.
- (15) Legare, S.; Lague, P. The influenza fusion peptide promotes lipid polar head intrusion through hydrogen bonding with phosphates and N-terminal membrane insertion depth. *Proteins: Struct., Funct., Bioinf.* **2014**, 82, 2118–2127.
- (16) Mirjanian, D.; Dickey, A. N.; Hoh, J. H.; Woolf, T. B.; Stevens, M. J. Splaying of Aliphatic Tails Plays a Central Role in Barrier Crossing during Liposome Fusion. *J. Phys. Chem. B* **2010**, 114, 11061–11068.
- (17) Fuhrmans, M.; Marrink, S. J. Molecular View of the Role of Fusion Peptides in Promoting Positive Membrane Curvature. *J. Am. Chem. Soc.* **2012**, 134, 1543–1552.
- (18) Huang, Q.; Chen, C. L.; Herrmann, A. Bilayer conformation of fusion peptide of influenza virus hemagglutinin: A molecular dynamics simulation study. *Biophys. J.* **2004**, 87, 14–22.
- (19) Li, J. Y.; Das, P.; Zhou, R. H. Single Mutation Effects on Conformational Change and Membrane Deformation of Influenza Hemagglutinin Fusion Peptides. *J. Phys. Chem. B* **2010**, 114, 8799–8806.
- (20) Bechor, D.; Ben-Tal, N. Implicit solvent model studies of the interactions of the influenza hemagglutinin fusion peptide with lipid bilayers. *Biophys. J.* **2001**, 80, 643–655.
- (21) Jang, H.; Michaud-Agrawal, N.; Johnston, J. M.; Woolf, T. B. How to lose a kink and gain a helix: pH independent conformational changes of the fusion domains from influenza hemagglutinin in heterogeneous lipid bilayers. *Proteins: Struct., Funct., Bioinf.* **2008**, 72, 299–312.
- (22) Panahi, A.; Feig, M. Conformational Sampling of Influenza Fusion Peptide in Membrane Bilayers as a Function of Termini and Protonation States. *J. Phys. Chem. B* **2010**, 114, 1407–1416.
- (23) Brice, A. R.; Lazaridis, T. Structure and dynamics of a fusion peptide helical hairpin on the membrane surface: Comparison of molecular simulations and NMR. *J. Phys. Chem. B* **2014**, 118, 4461–4470.
- (24) Haria, N. R.; Monticelli, L.; Fraternali, F.; Lorenz, C. D. Plasticity and conformational equilibria of influenza fusion peptides in model lipid bilayers. *Biochim. Biophys. Acta* **2014**, 1838, 1169–1179.
- (25) Baker, M. K.; Gangupomu, V. K.; Abrams, C. F. Characterization of the water defect at the HIV-1 gp41 membrane spanning domain in bilayers with and without cholesterol using molecular simulations. *Biochim. Biophys. Acta* **2014**, 1838, 1396–1405.
- (26) Barz, B.; Wong, T. C.; Kosztin, I. Membrane curvature and surface area per lipid affect the conformation and oligomeric state of HIV-1 fusion peptide: A combined FTIR and MD simulation study. *Biochim. Biophys. Acta* **2008**, 1778, 945–953.
- (27) Kamath, S.; Wong, T. C. Membrane structure of the human immunodeficiency virus gp41 fusion domain by molecular dynamics simulation. *Biophys. J.* **2002**, 83, 135–143.

- (28) Langham, A.; Kaznessis, Y. Simulation of the N-terminus of HIV-1 glycoprotein 41000 fusion peptide in micelles. *J. Pept. Sci.* **2005**, *11*, 215–224.
- (29) Taylor, A.; Sansom, M. S. P. Studies on viral fusion peptides: The distribution of lipophilic and electrostatic potential over the peptide determines the angle of insertion into a membrane. *Eur. Biophys. J.* **2010**, *39*, 1537–1545.
- (30) Wong, T. C. Membrane structure of the human immunodeficiency virus gp41 fusion peptide by molecular dynamics simulation II. The glycine mutants. *Biochim. Biophys. Acta* **2003**, *1609*, 45–54.
- (31) Risselada, H. J.; Marelli, G.; Fuhrmans, M.; Smirnova, Y. G.; Grubmüller, H.; Marrink, S. J.; Müller, M. Line-Tension Controlled Mechanism for Influenza Fusion. *PLoS One* **2012**, *7*, No. e38302.
- (32) Berendsen, H. J. C.; van der Spoel, D.; van Drunen, R. GROMACS: A message-passing parallel molecular-dynamics implementation. *Comput. Phys. Commun.* **1995**, *91*, 43–56.
- (33) Hess, B.; Kutzner, C.; van der Spoel, D.; Lindahl, E. GROMACS 4: Algorithms for highly efficient, load-balanced, and scalable molecular simulation. *J. Chem. Theory Comput.* **2008**, *4*, 435–447.
- (34) Schmid, N.; Eichenberger, A. P.; Choutko, A.; Riniker, S.; Winger, M.; Mark, A. E.; van Gunsteren, W. F. Definition and testing of the GROMOS force-field versions 54A7 and 54B7. *Eur. Biophys. J.* **2011**, *40*, 843–856.
- (35) Hermans, J.; Berendsen, H. J. C.; van Gunsteren, W. F.; Postma, J. P. M. A consistent empirical potential for water–protein interactions. *Biopolymers* **1984**, *23*, 1513–1518.
- (36) Poger, D.; Van Gunsteren, W. F.; Mark, A. E. A New Force Field for Simulating Phosphatidylcholine Bilayers. *J. Comput. Chem.* **2010**, *31*, 1117–1125.
- (37) Chiu, S. W.; Clark, M.; Balaji, V.; Subramaniam, S.; Scott, H. L.; Jakobsson, E. Incorporation of Surface Tension into Molecular Dynamics Simulation of an Interface—A Fluid Phase Lipid Bilayer Membrane. *Biophys. J.* **1995**, *69*, 1230–1245.
- (38) Miyamoto, S.; Kollman, P. A. SETTLE: An analytical version of the SHAKE and RATTLE algorithm for rigid water models. *J. Comput. Chem.* **1992**, *13*, 952–962.
- (39) Hess, B.; Bekker, H.; Berendsen, H. J. C.; Fraaije, J. G. E. M. LINCS: A linear constraint solver for molecular simulations. *J. Comput. Chem.* **1997**, *18*, 1463–1472.
- (40) Berendsen, H. J. C.; Postma, J. P. M.; van Gunsteren, W. F.; Dinola, A.; Haak, J. R. Molecular dynamics with coupling to an external bath. *J. Chem. Phys.* **1984**, *81*, 3684–3690.
- (41) van Gunsteren, W. F.; Berendsen, H. J. C. Computer simulation of molecular dynamics: Methodology, applications, and perspectives in chemistry. *Angew. Chem., Int. Ed. Engl.* **1990**, *29*, 992–1023.
- (42) Tironi, I. G.; Sperb, R.; Smith, P. E.; van Gunsteren, W. F. A generalized reaction field method for molecular dynamics simulations. *J. Chem. Phys.* **1995**, *102*, 5451–5459.
- (43) Smith, P. E.; Pettitt, B. M. Modeling Solvent in Biomolecular Systems. *J. Phys. Chem.* **1994**, *98*, 9700–9711.
- (44) Rafalski, M.; Ortiz, A.; Rockwell, A.; Vanginkel, L. C.; Lear, J. D.; Degrado, W. F.; Wilschut, J. Membrane-Fusion Activity of the Influenza Virus Hemagglutinin—Interaction of Ha2 N-Terminal Peptides with Phospholipid Vesicles. *Biochemistry* **1991**, *30*, 10211–10220.
- (45) Durrer, P.; Galli, C.; Hoenke, S.; Corti, C.; Glück, R.; Vorherr, T.; Brunner, J. H<sup>+</sup>-induced membrane insertion of influenza virus hemagglutinin involves the HA2 amino-terminal fusion peptide but not the coiled coil region. *J. Biol. Chem.* **1996**, *271*, 13417–13421.
- (46) Haque, M. E.; Koppaka, V.; Axelsen, P. H.; Lentz, B. R. Properties and structures of the influenza and HIV fusion peptides on lipid membranes: Implications for a role in fusion. *Biophys. J.* **2005**, *89*, 3183–3194.
- (47) Farrotti, A.; Bocchinfuso, G.; Palleschi, A.; Rosato, N.; Salnikow, E. S.; Voievoda, N.; Bechinger, B.; Stella, L. Molecular dynamics methods to predict peptide locations in membranes: LAH4 as a stringent test case. *Biochim. Biophys. Acta* **2015**, *1848*, 581–592.
- (48) Esteban-Martin, S.; Salgado, J. Self-assembling of peptide/membrane complexes by atomistic molecular dynamics simulations. *Biophys. J.* **2007**, *92*, 903–912.
- (49) Lorieau, J. L.; Louis, J. M.; Bax, A. Whole-Body Rocking Motion of a Fusion Peptide in Lipid Bilayers from Size-Dispersed <sup>15</sup>N NMR Relaxation. *J. Am. Chem. Soc.* **2011**, *133*, 14184–14187.
- (50) Lague, P.; Roux, B.; Pastor, R. W. Molecular dynamics simulations of the influenza hemagglutinin fusion peptide in micelles and bilayers: Conformational analysis of peptide and lipids. *J. Mol. Biol.* **2005**, *354*, 1129–1141.
- (51) Vaccaro, L.; Cross, K. J.; Kleinjung, J.; Straus, S. K.; Thomas, D. J.; Wharton, S. A.; Skehel, J. J.; Fraternali, F. Plasticity of influenza haemagglutinin fusion peptides and their interaction with lipid bilayers. *Biophys. J.* **2005**, *88*, 25–36.
- (52) Allen, W. J.; Lemkul, J. A.; Bevan, D. R. GridMAT-MD: A Grid-Based Membrane Analysis Tool for Use with Molecular Dynamics. *J. Comput. Chem.* **2009**, *30*, 1952–1958.
- (53) Lau, W. L.; Ege, D. S.; Lear, J. D.; Hammer, D. A.; DeGrado, W. F. Oligomerization of fusogenic peptides promotes membrane fusion by enhancing membrane destabilization. *Biophys. J.* **2004**, *86*, 272–284.
- (54) Poger, D.; Mark, A. E. On the Validation of Molecular Dynamics Simulations of Saturated and *cis*-Monounsaturated Phosphatidylcholine Lipid Bilayers: A Comparison with Experiment. *J. Chem. Theory Comput.* **2010**, *6*, 325–336.